T. B. Strayer

OBSERVATIONS OF WHISTLERS FROM JUPITER BY VOYAGER 1

by

Brian Dean Strayer

A thesis submitted in partial fulfillment
of the requirements for the degree of
Master of Science in Physics
in the Graduate College of
The University of Iowa

May, 1981

Thesis supervisor: Professor Donald A. Gurnett

Graduate College
The University of Iowa
Iowa City, Iowa

CERTIFICATE OF APPROVAL

MASTER'S THESIS

This is to certify that the Master's thesis of

Brian Dean Strayer

has been approved by the Examining Committee for the thesis requirement for the Master of Science degree in Physics at the May, 1981 graduation.

Thesis committee: Donald A. Gurnett
Thesis supervisor

Wm W. Kleiv
Member

Stanley D. Shawhan
Member

ACKNOWLEDGMENTS

A work of this complexity and size is rarely completed by one individual. Help can be received from others in a great many ways. Aside from the more obvious aspects of the drafting work and typing, there is an untold number of hours given by colleagues for consultation and explanation. In the instance of this particular paper, there is a long list of individuals to which thanks must be given.

The most important acknowledgment is made to Professor Donald A. Gurnett who not only supplied the idea for this study, but gave the author the opportunity to perform the necessary research to satisfy the degree requirements. Thanks are also given to Professor Stanley D. Shawhan for his guidance through the final version of the paper and to Professor W. H. Klink for useful criticisms which provided an objective view. Recognition of Dr. Roger R. Anderson's time provided in explaining the data processing and analysis necessary for the research is given as well. Most of all, the author wishes to extend the greatest appreciation to Dr. William S. Kurth. His door was always open when problems arose and his encouragement provided the motivation and supported the optimism necessary to bring the project through to its completion.

The excellent graphics work is primarily the result of the efforts of "Big John" Birkbeck whose suggestions gave the figures their optimal clarity and whose willingness to work on the figures, especially near deadlines, exceeded all expectations. Jeana Wonderlich also provided valuable illustrating assistance.

Thanks must also be given to Mr. R. West, Mrs. Dora Walker, Mr. Mark Brown, and Mr. Larry Granroth for performing much of the very time-consuming data processing work.

The efficient and accurate typing services of Alice Shank that permitted the timely submission of this thesis are gratefully recognized.

Finally, the author is extremely grateful for the atmosphere conductive to higher learning that exists within the Department of Physics and Astronomy and the University of Iowa as a whole.

This research was supported by NASA through Contract 954013 with the Jet Propulsion Laboratory and through Grant NGL-16-001-043 with NASA Headquarters. The support of the Office of Naval Research is also to be recognized with great appreciation.

ABSTRACT

Whistlers were observed in the wideband data from the plasma wave experiment during the Voyager 1 encounter of Jupiter. In a nine hour period near closest approach a total of 167 whistlers, 90 of which were suitable for study, were found to occur in three distinct regions. No recognizable whistlers were observed outside of ~ 6 R_J or on L-shells within the inner edge of the Io plasma torus. Two of the three regions in which whistlers were observed are in the northern portion of the torus. Five whistlers with dispersions on the order of 275 sec $Hz^{1/2}$ comprised the first group observed and travelled through a much larger portion of the torus than the second group. The second group, consisting of 79 whistlers, was located in the region of the cold torus core and mainly had dispersions ranging from 50 sec $Hz^{1/2}$ to 70 sec $Hz^{1/2}$. The six members of the third group were observed in the southern portion of the torus and had dispersions between 390 sec $Hz^{1/2}$ and 560 sec $Hz^{1/2}$ indicating their passage was through the bulk of the torus. The southern hemisphere appears to be the source of the whistlers in the first group while the northern hemisphere has the most evidence supporting it as the source for the second and third groups. The magnetic field lines passing through the whistler regions were

traced back to the planet's surface and indicated possible source regions for the whistlers at ~ 52°, ~ -71°, and ~ 76° latitude. A calculation of whistler amplitudes shows their peak intensities to be on the order of 30 μVm^{-1}. Analyses of the upper and lower whistler cutoff frequencies indicate a plasma temperature in parts of the torus as high as $(2 - 3) \times 10^5$ °K.

TABLE OF CONTENTS

LIST OF FIGURES

I. INTRODUCTION

The Voyager 1 spacecraft includes a plasma wave instrument which provides measurements of low frequency plasma waves (10 Hz to 56 kHz). During the Voyager 1 encounter of Jupiter, a number of lightning-generated whistlers were identified in the electric field waveform measurements made by this instrument [Gurnett et al., 1979]. Whistlers are identified by the frequency-time variation of their signal. A formula first posed by Eckersley [1935] describes the dispersion properties of whistlers

$$t = D/\sqrt{f} + t_o \quad ,$$

where t is the arrival time of a specific frequency f, and D is a constant known as the dispersion. Figure 1 shows two clearly defined whistlers. The first has a dispersion equal to 290 sec $Hz^{1/2}$ while that of the second is 275 sec $Hz^{1/2}$. Whistlers propagate at frequencies below the electron gyrofrequency and are guided along magnetic field lines from one hemisphere to the other. An extensive explanation of the whistler phenomena is given by Helliwell [1965].

This thesis is intended to give a concise compilation of whistler dispersions, rates of occurrence, and locations of all whistlers observed during the Voyager 1 flyby of Jupiter. A discussion as to the possible source regions of the whistlers is presented. Additionally, calculations of whistler peak intensities are performed, a rough approximation of the Io plasma torus temperature is made, and the question of whether or not a region of preference exists for whistler propagation through the magnetosphere is considered.

In understanding the whistler analysis process, a brief description of the plasma wave system on board Voyager 1 is appropriate. Electric field signals received by the antennas pass through a preamplifier and then a differential amplifier which provides an output proportional to the voltage difference between the two antennas. The signals are then processed in two ways: (1) by a 16-channel spectrum analyzer; and (2) by a waveform amplifier. The 16-channel spectrum analyzer lacks sufficient frequency and temporal resolution for whistler analysis, but provides absolute spectral density information used later in this study. High resolution frequency-time measurements of electric field waveforms were provided by the waveform amplifier. The bandwidth of these measurements is limited to the range 50 Hz to 10 kHz by a bandpass filter. An automatic gain control circuit comprises the waveform amplifier and maintains a constant output amplitude independent of the input

signal amplitude. Because the output amplitude is constant, absolute whistler peak intensities cannot be obtained from the waveform data alone. This is an important limitation discussed extensively later in this thesis. The waveform amplifier output is processed at a rate of 28,800 samples/sec by a 4-bit A/D converter and the 115.2 kbps output is recorded by the spacecraft data storage system. The telemetry system down link is shared with the imaging system providing the advantage of high rate data transmission but the disadvantage of limiting waveform data transmissions to selected periods. For a more extensive description of the instrumentation, see Scarf and Gurnett [1977].

II. OBSERVATIONS

A. Extent of Observation and Method of Measurement

Figure 2 shows the trajectory of Voyager 1 during the 14 hours of closest approach. The time period chosen for the study begins at 6:16:24 UT and ends at 15:08:41 UT. The original proposal of the study included time after 15:08:41 UT but data are not available between 15:08:41 UT and 19:45 UT. The digital wideband data are received in 48-second frames and are converted to analog frequency-time spectrograms. In all, 141 frames, representing 21% of the time period, are available for whistler detection. The three regions marked as A, B, and C represent periods where whistlers were detected. Figure 3 shows the relative scale of the distance to the region where whistlers from Jupiter are observed compared to the distance to the region where Earth-produced whistlers occur.

Whistler dispersions were determined by taking frequency and time measurements from the individual whistlers which were displayed in frequency-time spectrograms such as the one in Figure 1 and applying the Eckersley formula. An average of five pairs of measurements were taken directly from the spectrograms for each whistler having a dispersion greater than 100 sec $Hz^{1/2}$ and the mean of the dispersion calculations for each was used in the study. To

determine the dispersion of whistlers under 100 sec $Hz^{1/2}$ a transparency was created with whistlers drawn on it with dispersions from 20 sec $Hz^{1/2}$ to 100 sec $Hz^{1/2}$ at 5 sec $Hz^{1/2}$ intervals. The transparency was laid over the spectrograms and the whistlers were then matched to the nearest curve. Dispersions of whistlers could be read to within ± 2 sec $Hz^{1/2}$ which meant that the percent deviations from the actual values were at most 4% for whistlers with dispersions equal to 50 sec $Hz^{1/2}$ and 3% for whistlers with dispersions equal to 70 sec $Hz^{1/2}$. Percent deviations about the mean for whistlers having dispersions greater than 100 sec $Hz^{1/2}$ were less than 2%. It should be noted that the Eckersley formula is an approximation but its use is well within the accuracy constraints of this study for the range of whistler frequencies under investigation [Menietti and Gurnett, 1980].

A total number of 167 whistlers were identified in the data, 90 of which were used in the study. The other 77 lacked sufficient temporal and/or frequency extent to allow reliable dispersion measurements. Although they were not included in the dispersion statistics, the magnitudes of their dispersions were judged to be on the same order as the dispersion values for the analyzed whistlers within the same time interval.

B. Region of Occurrence

1. Jupiter as Source

The analysis now turns to a determination of the likely source regions for the whistlers. Although Jupiter is generally accepted as the source of all observed whistlers, the claim demands some proof because Io could be capable of producing whistlers. Io is recognized as a possible source because it has active volcanoes [Smith et al., 1979] and volcanoes on Earth have produced lightning which infers the possibility of lightning on Io. Gurnett et al. [1979] was able to demonstrate that Jupiter is the source of the whistlers. Two observations provide the key evidence. First, the lightning source is known to lie somewhere near the magnetic field line through the spacecraft because the whistler mode ray path cannot vary more than 19° from the local magnetic field [Helliwell, 1965]. Regarding the whistlers in regions A and B of Figure 2, only Jupiter was in the whistler mode propagation cone. Jupiter and Io lie within the propagation cone for whistlers in region C. Here again, Jupiter is accepted as the source not only because it must be the source to explain the presence of the whistlers in regions A and B, but because the whistler intensities for the two regions, as approximated by Gurnett et al. [1979], are both on the order of $30\ \mu Vm^{-1}$.

2. Northern and Southern Hemispheres as Points of Origin

The question of the whistler source region now centers on deciding which hemisphere the whistlers originate from. Figure 4 provides a guideline for this discussion. The whistlers in region A have dispersions on the order of 250 sec $Hz^{1/2}$. Figure 1 has two clear examples of whistlers with that approximate dispersion value. Region B contains whistlers having much smaller dispersions than those in A. The range of dispersions is primarily between 50 sec $Hz^{1/2}$ and 70 sec $Hz^{1/2}$ for whistlers of region B. See Figure 5 for examples of region B whistlers. Whistlers in region C have large dispersions on the order of 500 sec $Hz^{1/2}$. Figure 6 shows two region C whistlers. It is important to note the differences in the time scales of the three whistler figures in order to see the relative dispersion sizes. The range of dispersions for all measured whistlers is represented in the lower panel of Figure 7. Because no whistlers were found in the data from 0617 UT to 0900 UT, that period was dropped from the figure to allow a more detailed scale. Also, the whistler occurrence rate was so high at times, up to 32 per 48 second frame, that whistlers within 40 seconds of each other were averaged into single data points. Only whistlers of similar dispersion were averaged as groups. The error bars represent the standard deviation. The important point to notice in Figure 7 is the fluctuation of dispersion values among the whistlers in all three of the regions. Whistlers occurring within seconds of

another have differences in dispersions as large as 40%. This, coupled with the fact that there is no regular pattern among the dispersion shifts, indicates that the density within the torus may have large scale irregularities. Figure 8 shows in histogram form the number of whistlers in regions A, B, and C.

Before we can hypothesize on the possible source regions, two other pieces of relevant information must be added to the analysis. First, it is established that the dispersion of whistlers increases with both distance of propagation along the ray path and density of the medium traversed. Secondly, the whistlers are detected in the region of the Io plasma torus whose existence has been established with planetary radio astronomy measurements [Warwick et al., 1979] and with the ultraviolet spectrometer [Broadfoot et al., 1979]. The Io plasma torus is the primary cause of the whistler dispersions. Based on ray tracing calculations, it has been found that the contribution to the overall dispersion value of any given whistler by Jupiter's ionosphere and magnetosphere is only on the order of 4 or 5 sec $Hz^{1/2}$ [D. A. Gurnett, private communication, 1981]. This contribution is negligible compared to the measured dispersion values.

Thus it is apparent that the whistlers of region A should have a higher dispersion since they have traversed a denser region through the torus than those in B although the path length for whistlers of the two regions are not significantly different.

Referring again to Figure 4, the information of interest is the series of electron density contours taken from Bagenal et al. [1980]. Because of the irregular shape of the torus, whistlers in regions A and C traversed much more of the plasma region than whistlers of region B. A large temperature gradient exists at ~ 5.7 R_J with the high end away from Jupiter [Bagenal et al., 1980]. The higher temperatures outside of 5.7 R_J cause the torus to diffuse and create greater scale heights. Region A lies in the high temperature zone while region B is in the neighborhood of the cold torus core. Accepting these contours as accurate, we now see that even though the region B whistlers were observed within minutes of those in region A, the region A whistlers traversed a great deal more of the torus and thus have much greater dispersions. The fact that the spacecraft's trajectory is near the north boundary of the torus and the whistler dispersions are relatively small leads to the conclusion that the region B whistlers have their source in Jupiter's northern hemisphere. A conclusion is not as easily drawn for the whistlers of region A. The trajectory of Voyager 1 is only slightly north of the equatorial plane here. A case can be made for either hemisphere as being the source.

Recent information from Tokar et al. [1981] indicates that the region A whistlers have their source in the southern hemisphere. They calculated transit times by an integration of the group index of refraction along the field line from the lightning source to the

spacecraft. From the transit times they calculate a dispersion. An important assumption is made for the magnitude of the ion density. They have combined the plasma instrument (PLS) heavy-ion positive charge densities with estimated light-ion densities based on preserving local charge neutrality. The magnitude of a whistler's dispersion is dependent on the electron density of the region it traverses and the electron density is equal to the sum of the ion densities. Their calculations yield dispersions consistent with those of this study when the region B and C whistlers are treated as coming from the northern hemisphere and the region A whistlers are treated as coming from the southern hemisphere. The case for region C is the strongest. It is located well south of the equatorial plane and the whistlers found there have large relative dispersion sizes which further promotes the conclusion that these whistlers originated in Jupiter's northern hemisphere. The evidence points strongly toward the conclusion that whistlers emanate from both hemispheres although no lightning was visually observed in the southern hemisphere [Cook et al., 1979].

3. Point of Origin in Terms of Jovicentric Coordinates

An approximation as to the location of the source region on the planet's surface can be made by following the magnetic field lines that pass through the whistler regions back to the surface. Figure 9 shows a plot of the foot of the field line through Io

across a grid representing the planet's surface. The model used to determine the positioning of the foot of the Io field line is the Acuña and Ness [1976] O_4 model. The dark patches represent the probable source regions of the whistlers. Region A is shown as A1 and A2 because it has not been shown conclusively which hemisphere the region A whistlers have as their source. The latitudes for these probable source regions are ~ 48° for A1, ~ -71° for A2, ~ 52° for B, ~ 76° for C. The longitudes range from 209° - 217° for regions A1 and A2, 219° - 234° for region B, and 339° - 347° for region C.

C. Calculation of Whistler Intensities

Whistler peak amplitudes were calculated using the wideband data and the spectrum analyzer data. Nonaveraged plots of amplitude versus frequency were made of the wideband data. Figure 10 is an example. Note the whistler peak. The difficulty with the measurement lay in the fact that the amplitude scales do not have absolute values as a result of the AGC output being constant. To determine those absolute values, the spectrum analyzer output, which is absolute, was used. The spectrum analyzer makes a sweep through its 16 channels in a period of 4 seconds. Plots of amplitude versus frequency were made of the spectrum analyzer output for the time frames in which the observed whistlers were detected. These plots were then matched with wideband amplitude frequency plots that were averages of groups of 10 consecutive nonaveraged plots. Nonaveraged

plots have a time sweep of .06 sec. This matching process provided an absolute scale for the wideband data. The averaged plots were then matched with the nonaveraged plots in order to put an absolute value on the whistler peaks. The peak heights were read in units of spectral density ($V^2\ m^{-2}\ Hz^{-1}$). The calculation of whistler peak intensities involved multiplying the value for the whistler peak times the frequency half-width at half-height and then taking the square root. This produced the whistler peak intensity in the proper units of Vm^{-1}. Unfortunately, only two whistlers had signals that were differentiable from the background noise. Both were from region A and are the ones shown in Figure 1. The first whistler, with dispersion equal to 290 sec $Hz^{1/2}$, has a peak intensity of $\sim$ 27 μVm^{-1} at 3.3 kHz. The second whistler, with dispersion equal to 290 sec $Hz^{1/2}$, has a peak intensity of $\sim$ 39 μVm^{-1} at 4.5 kHz. The intensities are given at specific frequencies rather than integrated because the data are not complete enough for that calculation. Also, at any given instant in time, only a certain frequency width of the whistlers is visible in the data.

D. Region of Preferred Propagation

Going back to Figure 2 we see sizeable time periods where no whistlers were found in any of the frames available. Regions of preference either for whistler production at Jupiter or along the paths of propagation are possible explanations but other factors need to be considered closely before a conclusion can be founded.

To help explain the data void a plot of electric field strength over the 10 channels from 562 Hz to 10 kHz versus UT was produced (see Figure 11) and combined with a histogram of whistler occurrence versus UT. The main point to draw from this figure is that the whistlers are grouped in regions of low broadband noise. Where the noise was relatively high, whistlers were not found in the data. The possibility is recognized that whistlers may have been present where the spectral density is relatively high, but were overshadowed by the broadband noise. This is possible due to the effects of the automatic gain control in the plasma wave package. Since the AGC receiver output amplitude is virtually constant and independent of the input signal, signals in the same frequency range as the whistlers and with much greater intensity than the whistlers would command a correspondingly larger share of the output from the AGC. In this situation, the whistler signals would be overshadowed. To accommodate instantaneous fluctuations in the signal level, the A/D converter covers a dynamic range of +6 dB to -17 dB from the constant average output level. For that reason, the two whistlers with the computed peak intensities of 27 μVm^{-1} and 39 μVm^{-1}, respectively, were visible because the "dip" they coincide with in Figure 11 indicates a lower limit to the instrument's detection sensitivity at that time of 25 μVm^{-1}. The next "dip" in the integrated field strength curve where data are available and no whistlers are found has a lower limit of 37 μVm^{-1}. If we assume

that the two whistlers with measurable peak intensities have the largest intensities of all the whistlers, then it is clear that whistlers are probably not visible in the wideband data during periods other than the one they are presently found in because the waveform amplifier did not detect them. The large "dip" in Figure 11 corresponding to where the bulk of the whistlers are seen indicates a lower limit on the amplifier's sensitivity of 14 μVm^{-1} for that time period. Although no conclusion can be made as to whether or not a region of preference exists for whistler propagation, the indication here is that whistlers probably would have been seen in other regions had the background field intensities been low enough.

The highest background noise level of about 1000 μVm^{-1} occurred between 0600 and 0700 UT. Since whistlers could be detected down to 17 dB below this level, it is concluded that whistler amplitudes did not exceed 140 μVm^{-1} at any time during the Voyager 1 pass.

E. Io Torus Temperature Analysis

An approximation of the torus temperature along the field lines through the spacecraft where whistlers are found (between 5 and 6 R_J) can be made through an analysis of whistler low cutoff frequencies. The upper panel of Figure 7 gives whistler frequency ranges for all the whistlers studied. The same type of averaging process described in reference to the lower panel of Figure 7 was

used here as well. The upper panel of Figure 12 gives a blowup of the period 09:30 UT to 10:30 UT. Individual whistler frequency ranges are presented. Menietti and Gurnett [1980] are able to put an upper limit on the torus temperature with an investigation of Landau damping. Assuming the whistlers to be nonducted, the wave normal angle of a whistler will increase as it passes through the dense torus and Landau damping will occur. The general expression for collisionless damping given by Kennel [1966] is then applied and combined with a calculation of attenuations. To place an upper bound on the torus temperature, they use the lowest cutoff frequency of the whistlers which have passed through the bulk of the torus. The lowest cutoff frequency thus chosen is 1770 Hz as measured from a region A whistler. A cutoff in this range places an upper bound on the torus temperature of approximately $(2 - 3) \times 10^5$ °K [Menietti and Gurnett, 1980]. This is in fair agreement with the average time electron temperature of 10^5 °K calculated by Broadfoot et al. [1979] using the Voyager 1 ultraviolet spectrometer.

When constructing Figures 7 and 12 it was hoped that some sort of pattern in the data would become apparent. Perhaps the whistler dispersions would be seen to steadily increase with time or some type of consistent changes in frequency ranges would arise. Unfortunately, if a pattern does exist, it cannot be derived because the whistlers are not distributed sufficiently over space to provide one.

III. DISCUSSION

The study of dispersion, frequency, and intensity characteristics of whistlers passing through the Io torus has provided several important pieces of information. Based on relative dispersion sizes and electron density profiles of the Io torus, it was determined that the northern hemisphere is the most likely point of origin for the whistlers in regions B and C of Figure 4, while the southern hemisphere is the probable point of origin for the whistlers in region A. Computer generated dispersion values obtained from Tokar et al. [1981] for the three regions are in agreement with these point of origin determinations. The field lines through the whistler regions were traced back to the planet's surface and the whistlers of region A were found to emanate from either ~ -71° latitude, 209° - 217° longitude or +48° latitude, 209° - 217° longitude. Of the two possible source regions, the computer calculations favor them coming from ~ -71° latitude, 209° - 217° longitude. Whistlers of region B were found to emanate from ~ 52° latitude, 219° - 234° longitude, and those of region C from ~ 76° latitude, 339° - 347° longitude. Cook et al. [1979] observed a lightning activity between 45° and 55° latitude, 27° and 51° longitude. Figure 9 shows the locations of their observations in Jovicentric

coordinates. Although they only observed lightning activity in the northern hemisphere, it should be pointed out that their ability to observe the southern hemisphere was rather restricted. It is not possible to compare whistler points of origin directly with lightning activity because the lightning observations took place during a short time period approximately three hours after the last whistlers were observed. Since Jupiter rotation rate is on the order of 10 hours, Cook et al. [1979] had a quite different view of the planet from that which they would have had during the whistler observations (see Figure 9). Nonetheless, it is worth noting that the whistlers of region B, by far the largest group in terms of number, are in the same latitude range as the observed lightning activity.

Measurements of the peak intensities of two clearly defined whistlers gave values of 27 μVm^{-1} and 39 μVm^{-1}. These numbers are in good agreement with the earlier Gurnett et al. [1979] whistler intensity estimation of 30 μVm^{-1}. Assuming the 39 μVm^{-1} whistler peak intensity to be the strongest signal, it appears that the non-existence of whistler observations for extended time periods was a result of the relative size of the background field intensity rather than an indication that regions for preferred propagation exist (see Figure 11).

Menietti and Gurnett [1980] were able to put an upper limit on the torus electron temperature for regions in which whistlers

were found by applying some Landau damping theory to data involving whistler low frequency cutoffs. The value of 1770 Hz as the lowest cutoff for a long dispersion whistler gives an upper bound of $(2 - 3) \times 10^5$ °K which is in good agreement with the Broadfoot et al. [1979] average torus electron temperature calculation of 10^5 °K. Another point of interest gleaned from the data was that even though whistlers were found to occur at rapid rates in places with as many as 32 appearing in one 48-second frame, there was no evidence of multiple-hop whistlers. As an explanation, Menietti and Gurnett [1980] proposed that the vast majority of whistlers, including the ones in the study, are nonducted and therefore the Landau damping phenomena becomes very strong for those passing through the dense torus. After the first traversal of the equatorial plane, the whistler signals attenuate out and thus would not be detected as passing back through the torus.

Figure 1. A frequency-time spectrogram showing two distinct whistler signals. The ordinate axis represents frequency from 0 to 10 kHz. The abscissa is calibrated in seconds. The first whistler has a dispersion equal to 290 sec $Hz^{1/2}$ and the second one is equal to 275 sec $Hz^{1/2}$. This spectrogram begins at time 0912:48 UT.

B-G79-321

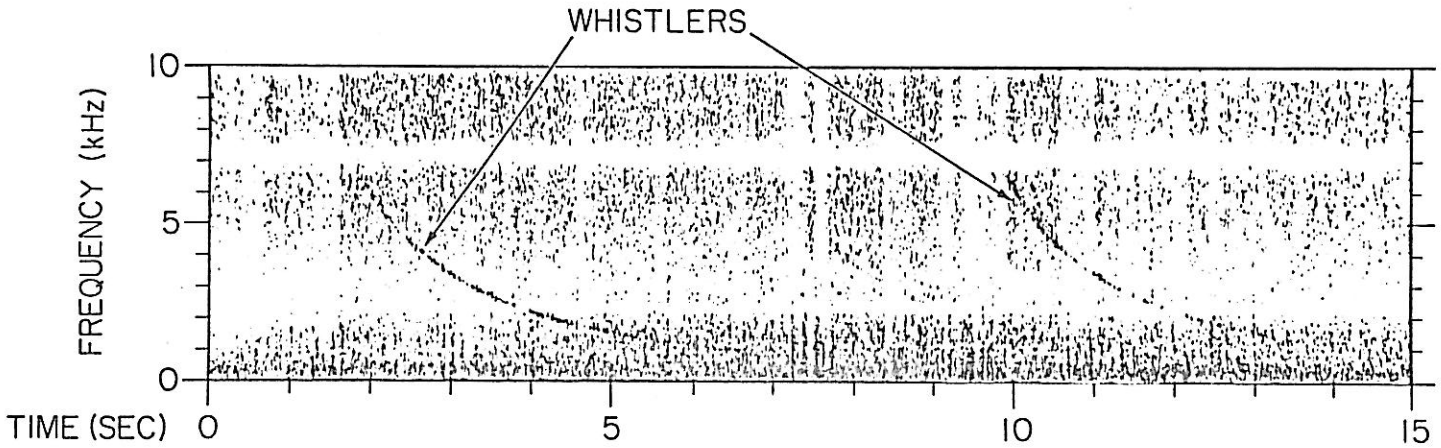

VOYAGER-1, START TIME, DAY 64, 0912:48.53 UT (SCET)

R = 5.80 R_J, LT = 16.4 HR, ϕ_{III} (1965) = 201.0°, λ_m = 5.45°

Figure 1

Figure 2. Trajectory of Voyager 1 during closest approach to Jupiter, March 5, 1979. Regions A, B, and C denote locations where whistlers were detected.

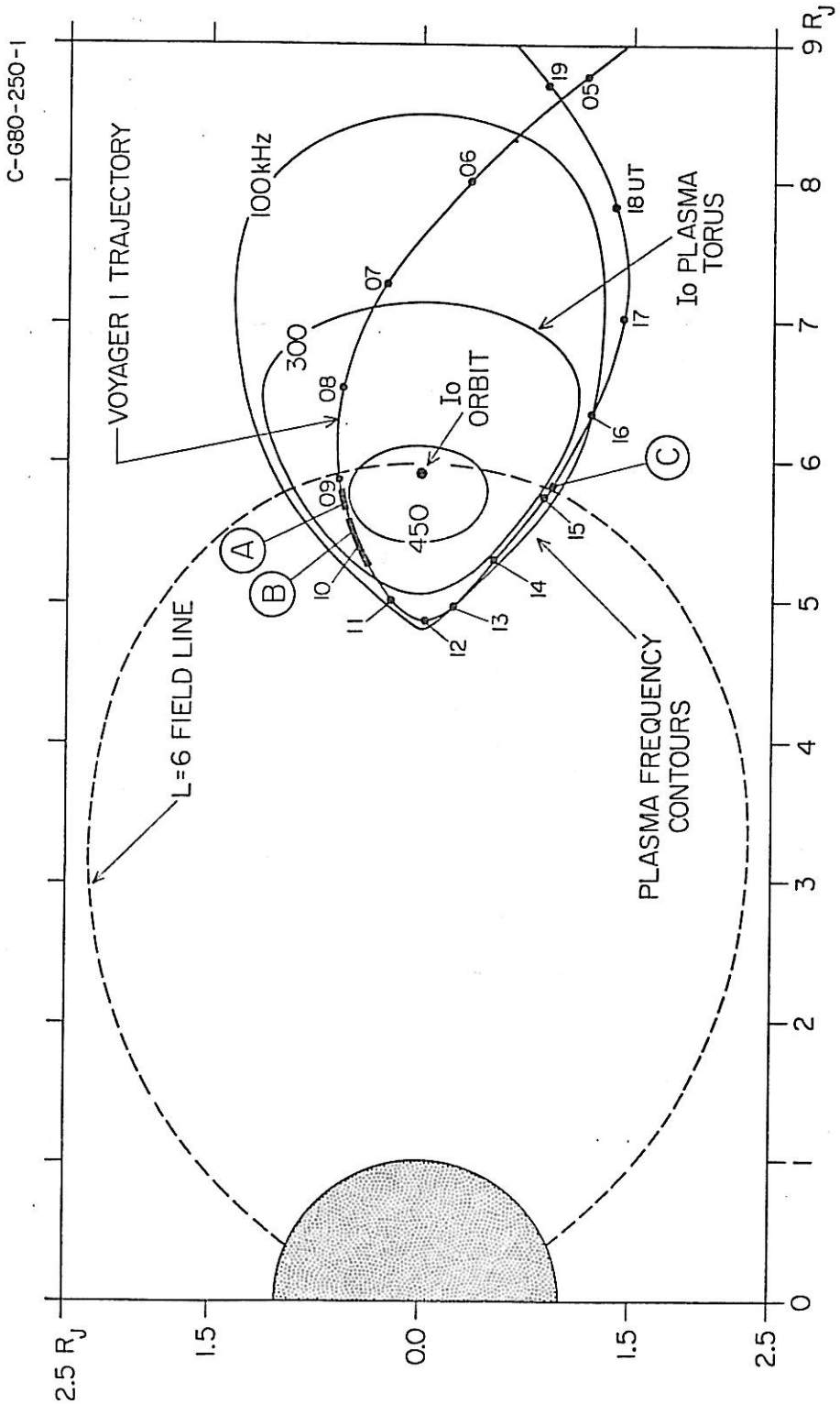
C-680-250-1
VOYAGER 1 TRAJECTORY
100 kHz
300
450
Io ORBIT
Io PLASMA TORUS
L=6 FIELD LINE
PLASMA FREQUENCY CONTOURS
A
B
C
05
06
07
08
09
10
11
12
13
14
15
16
17
18 UT
19
9 R_J
8
7
6
5
4
3
2
1
0
2.5 R_J
1.5
0.0
1.5
2.5

Figure 2

Figure 3. Diagram showing the relative distance out from Jupiter that whistlers were observed in relation to the distance from Earth that terrestrial whistlers have been observed. The locations of the Earth's plasmapause and bow shock are included to give more meaning to the scale.

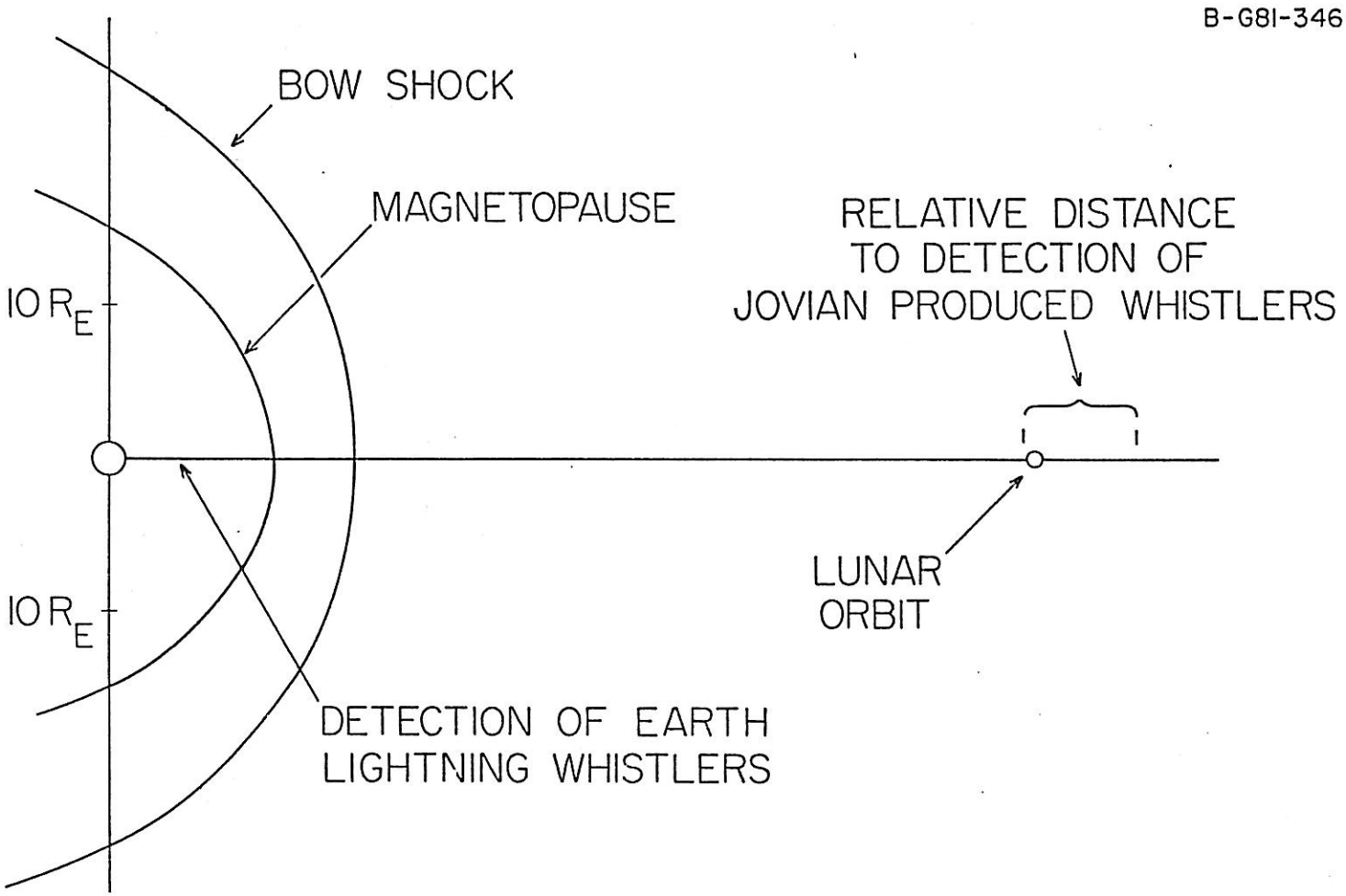
B-G81-346-1
BOW SHOCK
MAGNETOPAUSE
10 R_E
10 R_E
RELATIVE DISTANCE
TO DETECTION OF
JOVIAN PRODUCED WHISTLERS
LUNAR
ORBIT
DETECTION OF EARTH
LIGHTNING WHISTLERS

Figure 3

Figure 4. Trajectory of Voyager 1 during closest approach superimposed on the Bagenal et al. [1980] electron density contours. Contour levels are in steps of 200 cm^{-3}. Whistlers were detected in regions A, B, and C. Dispersions for whistlers in region A are on the order of 250 sec $Hz^{1/2}$. Whistlers in region B have dispersions predominately between 50 sec $Hz^{1/2}$ and 70 sec $Hz^{1/2}$ while those in region C are on the order of 500 sec $Hz^{1/2}$.

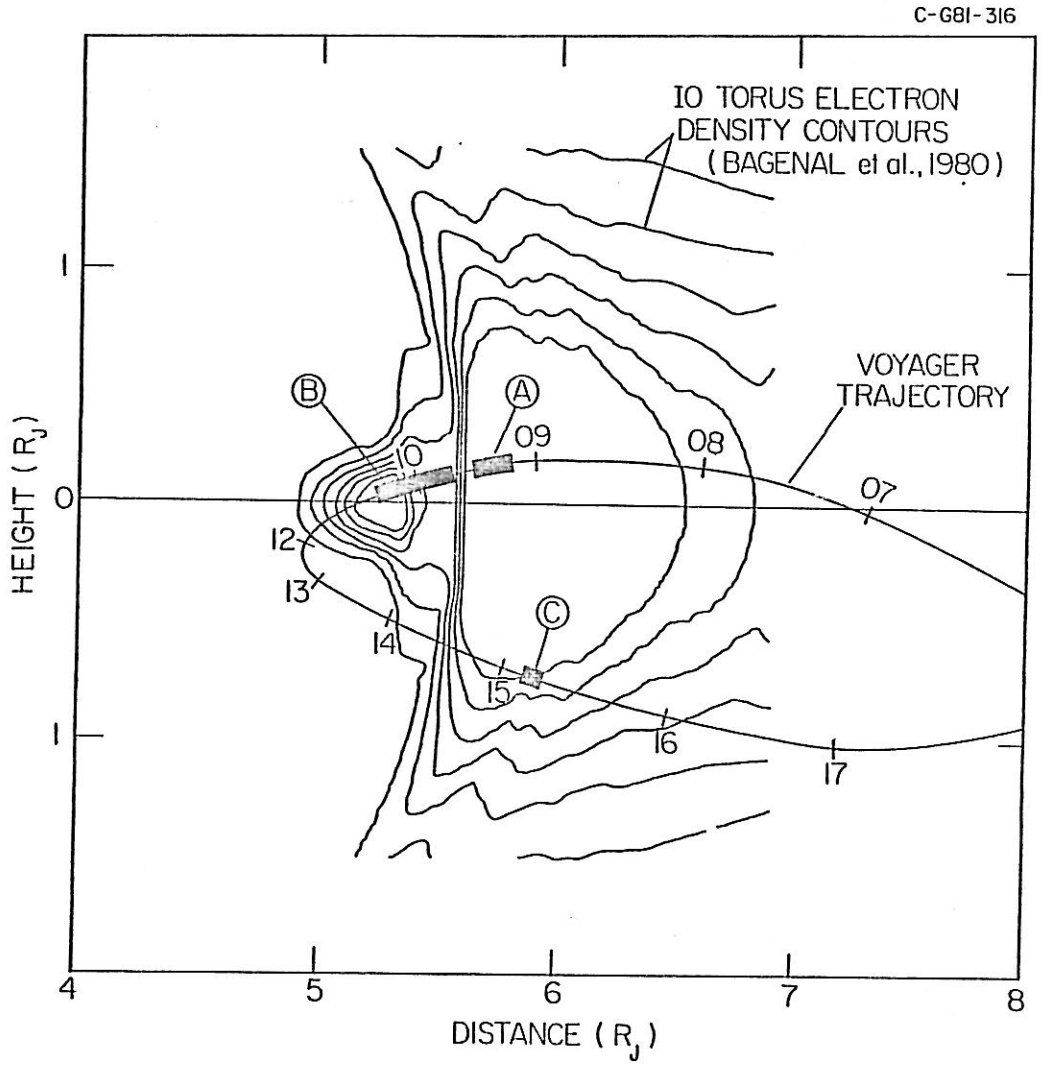
C-G81-316
IO TORUS ELECTRON
DENSITY CONTOURS
(BAGENAL et al., 1980)
VOYAGER
TRAJECTORY
HEIGHT (R_J)
DISTANCE (R_J)
1
0
1
4
5
6
7
8
A
B
C
10
09
08
07
12
13
14
15
16
17

Figure 4

Figure 5. A frequency-time spectrogram showing several whistler signals. The ordinate axis represents frequency from 0 to 7 kHz. The abscissa is calibrated in seconds. The time of the spectrogram begins at 1016:24.5 UT. The whistlers in the spectrogram have dispersions on the order of 45 sec $Hz^{1/2}$.

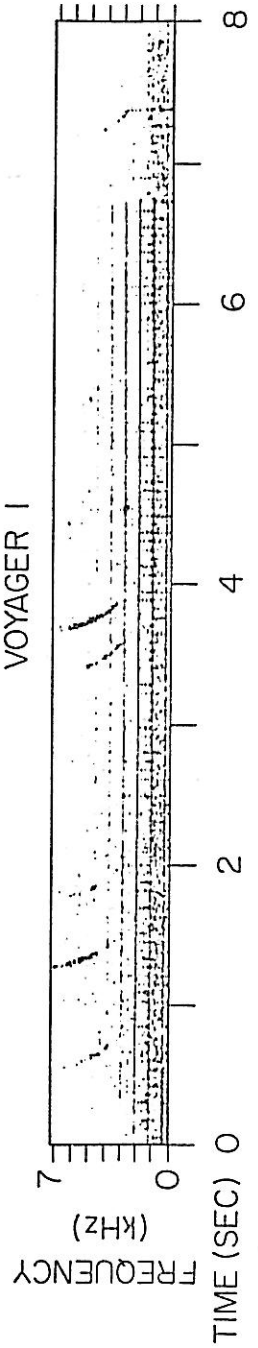
B-G80-531
VOYAGER 1
FREQUENCY (KHz)
7
0
TIME (SEC) 0
2
4
6
8
START TIME DAY 64, MARCH 5, 1979, 1016:24.5 UT
R = 5.3 R_J LT = 17.4 HR λ_m = 3.9°

Figure 5

Figure 6. A frequency-time spectrogram showing two distinct whistler signals. The ordinate axis represents frequency from 0 to 10 kHz. The abscissa is calibrated in seconds. The time of the spectrogram begins at 15:07:05 UT. The first whistler has a dispersion equal to 430 sec $Hz^{1/2}$ and the second one is equal to 477 sec $Hz^{1/2}$.

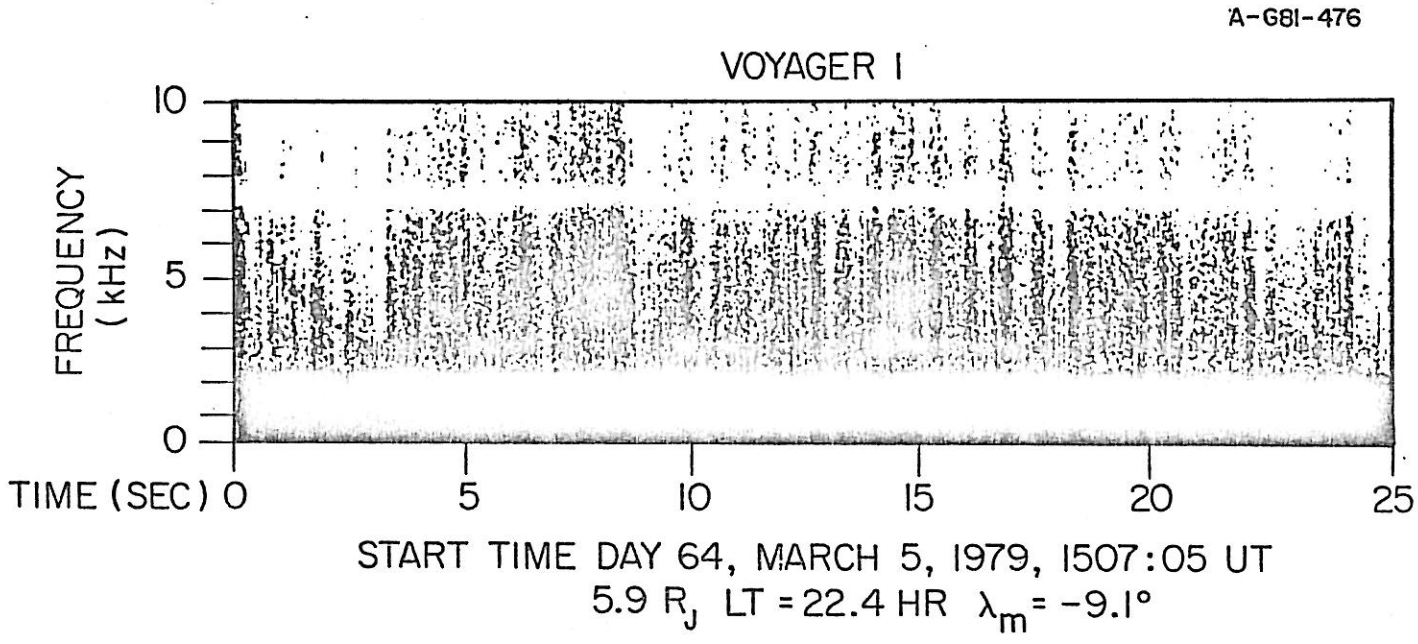
A-G81-476
VOYAGER 1
FREQUENCY (kHz)
10
5
0
TIME (SEC) 0
5
10
15
20
25
START TIME DAY 64, MARCH 5, 1979, 1507:05 UT
5.9 R_J LT = 22.4 HR λ_m = -9.1°

Figure 6

Figure 7. Upper panel: Frequency ranges for all whistlers used in the study versus UT. High and low frequency cutoffs for whistlers occurring within 40 seconds of one another were averaged so that data would fit the time scale. Numbers below lines represent line number of whistlers averaged to produce the line. The study begins at 06:17 UT but the time period preceding 0900 UT which contained no detectable whistler occurrences has been deleted to increase the clarity of the diagram. Thick ticks along the time axis denote periods where waveform data is available. Lower panel: Whistler dispersions versus UT for all whistlers used in the study. Dispersions of whistlers occurring within 40 seconds of one another have been averaged for the calculation of individual data points. Error bars denote the standard deviation.

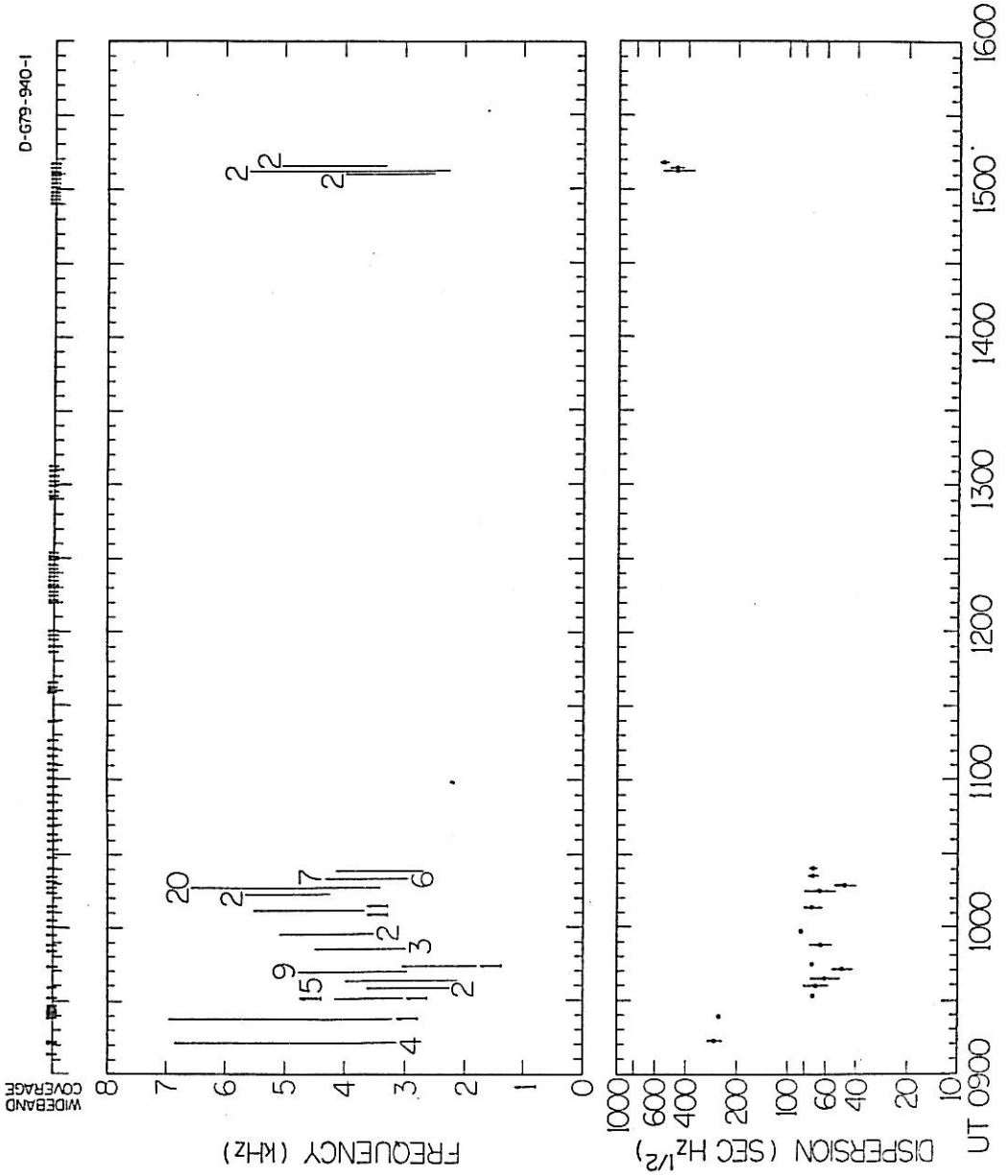
D-679-940-1
WIDEBAND COVERAGE
FREQUENCY (kHz)
DISPERSION (SEC Hz^1/2)
UT 0900
1000
1100
1200
1300
1400
1500
1600

Figure 7

Figure 8. Histogram of whistler occurrences versus dispersion. Note the representation of three distinct groups. The whistlers with dispersions less than 100 sec $Hz^{1/2}$ were detected in region B of Figure 4. Whistlers with dispersions between 200 sec $Hz^{1/2}$ and 300 sec $Hz^{1/2}$ correspond to region A and those with dispersions greater than 375 sec $Hz^{1/2}$ were observed in region C of Figure 4.

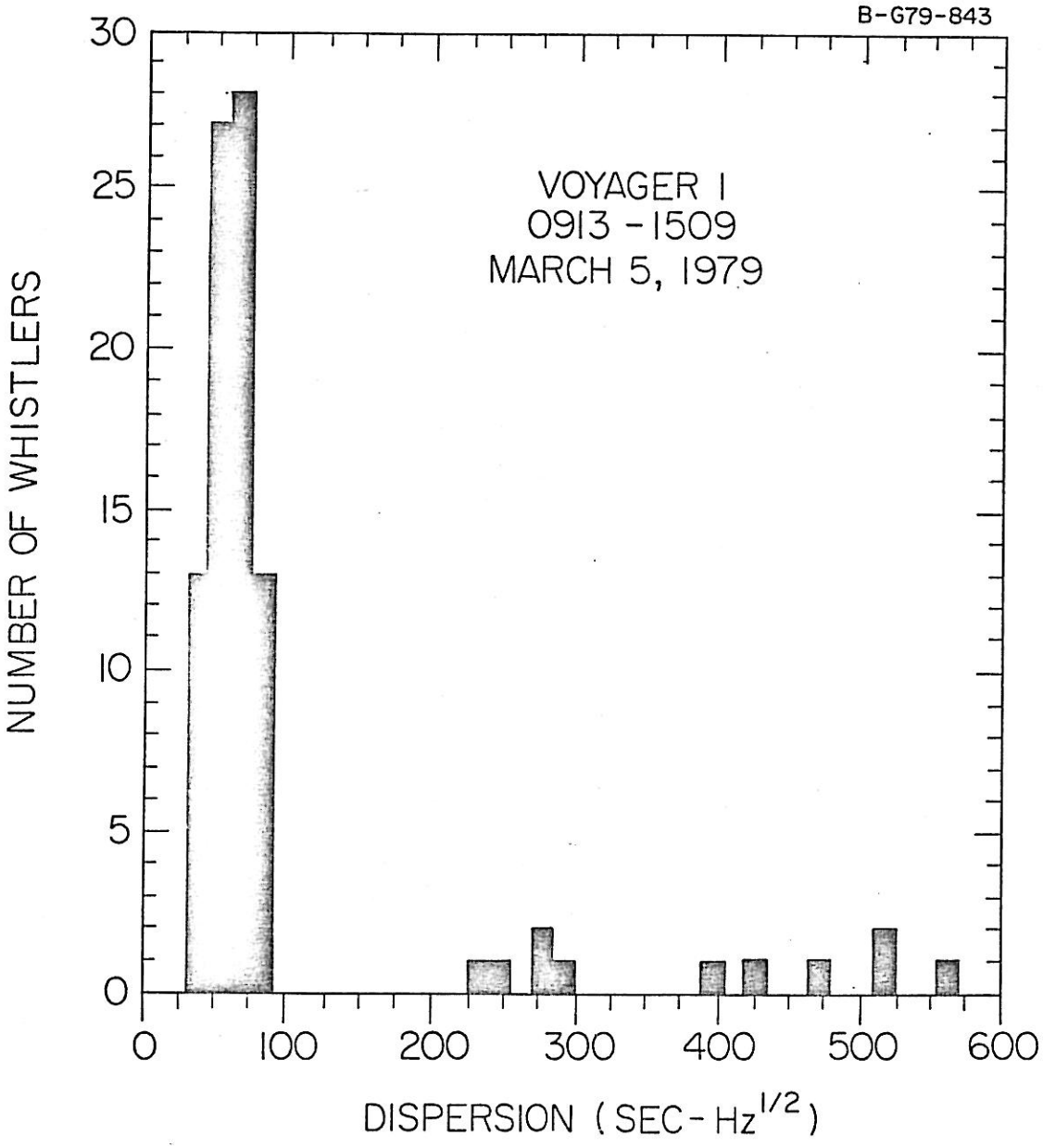
B-G79-843
VOYAGER 1
0913 - 1509
MARCH 5, 1979
NUMBER OF WHISTLERS
DISPERSION (SEC - Hz^1/2)
0
5
10
15
20
25
30
0
100
200
300
400
500
600

Figure 8

Figure 9. Jovicentric coordinate grid as represented in two dimensions. The dashed curves represent the foot of the field line passing through Io and were positioned in accordance with the Acuña and Ness [1976] Model O_4. Regions A, B, and C represent possible source regions of whistlers. The locations of visible lightning activity as detected by Cook et al. [1979] are in the upper right-hand corner.

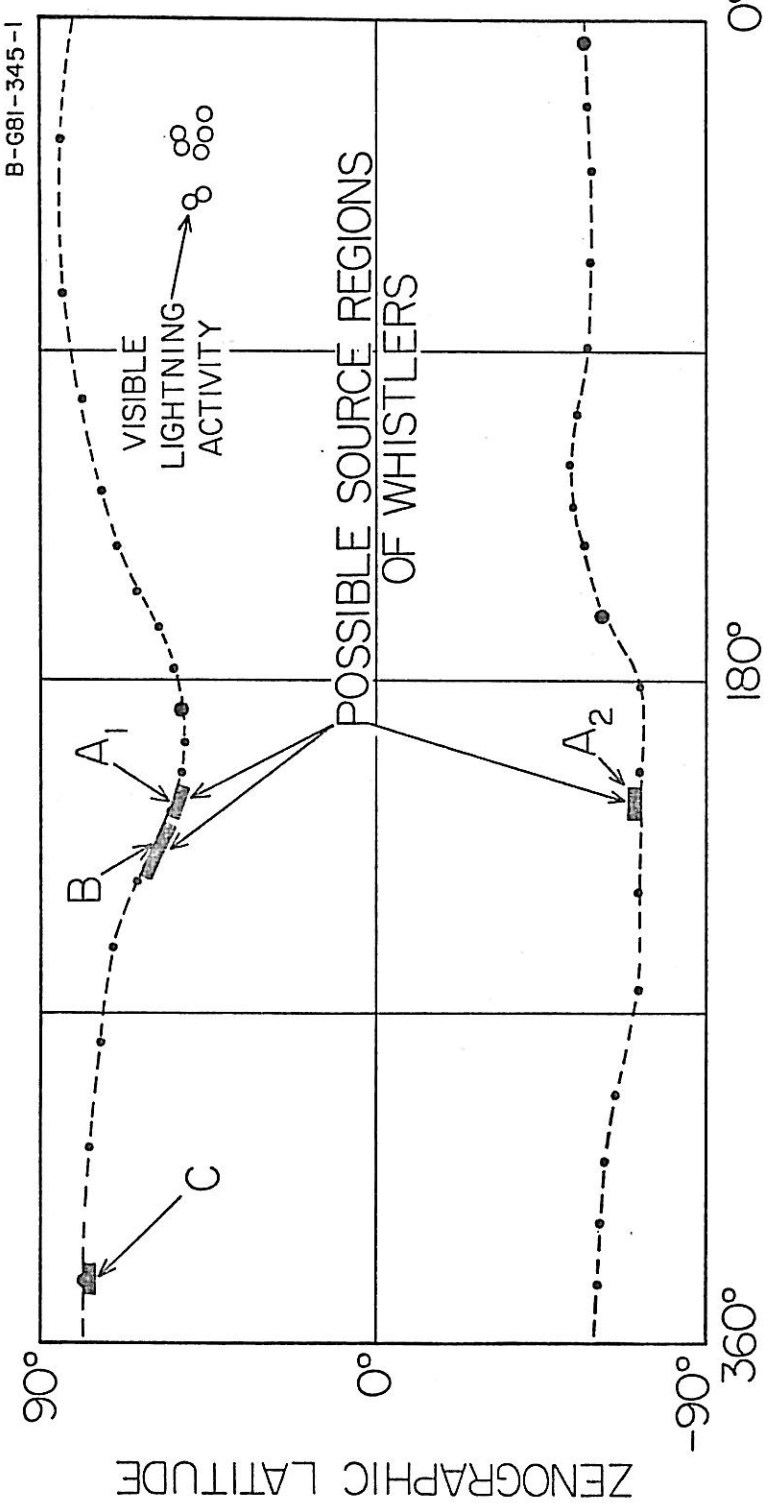
B-G81-345-1
VISIBLE LIGHTNING ACTIVITY
POSSIBLE SOURCE REGIONS OF WHISTLERS
A1
A2
B
C
90°
0°
-90°
0°
180°
360°
ZENOGRAPHIC LATITUDE
ZENOGRAPHIC LONGITUDE

Figure 9

Figure 10. An amplitude-frequency spectrogram from the wideband data. The ordinate axis represents spectral density in units of $V^2\ m^{-2}\ Hz^{-1}$. The abscissa is calibrated in kHz. The whistler signal is centered at 4.5 kHz, has an amplitude of 39 μVm^{-1}, and a dispersion equal to 275 sec $Hz^{1/2}$. The start time of the spectrogram is 0912:59.1 UT.

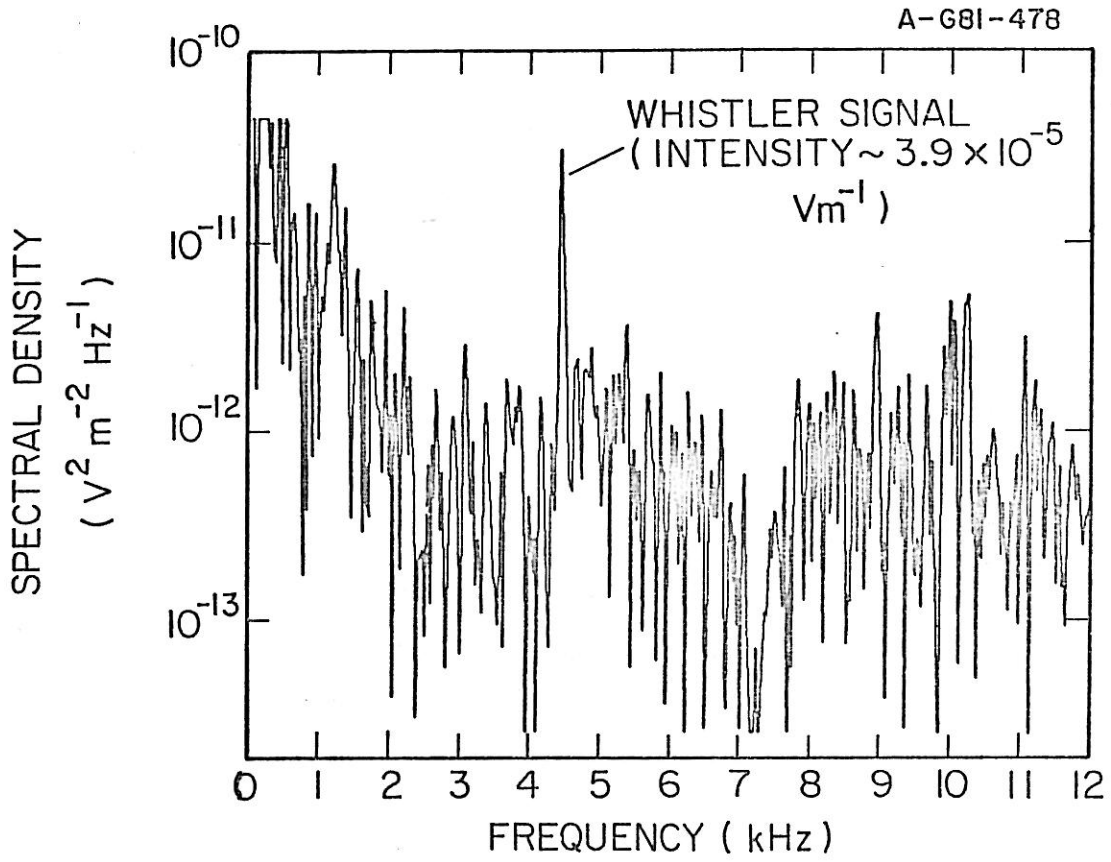

DAY 64, MARCH 5, 1979, 912:59.1 UT

REGION A, WHISTLER DISPERSION = 275 (SEC - $Hz^{1/2}$)

Figure 10

Figure 11. Upper panel: Histogram of whistler occurrences versus UT for time period 06:00 UT to 16:00 UT. Dots along lower time axis denote periods where waveform data is available. Lower panel: Plot of spectral density versus UT for time period 06:00 UT to 16:00 UT. (Note that whistlers are detected in regions of relatively low broadband noise.)

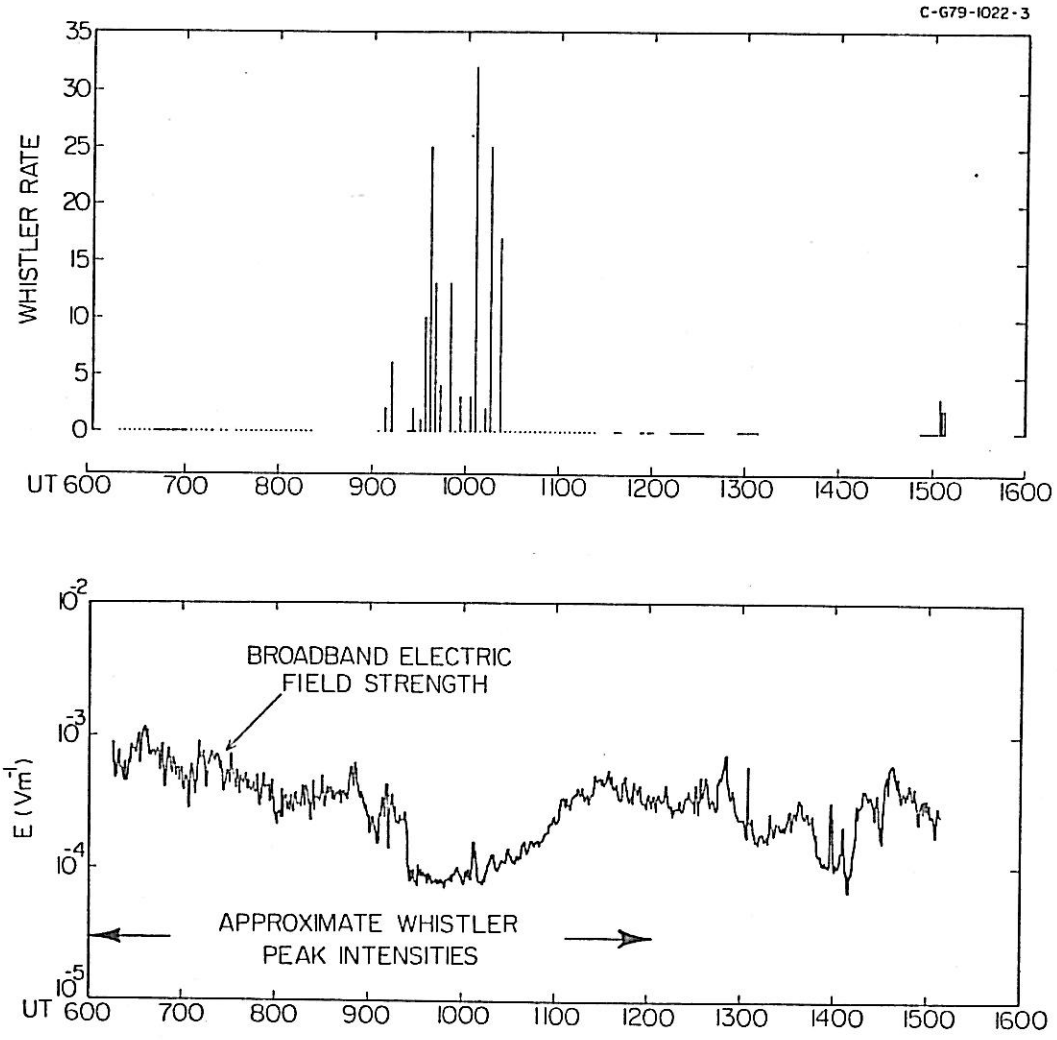
C-G79-1022-3
WHISTLER RATE
35
30
25
20
15
10
5
0
UT 600
700
800
900
1000
1100
1200
1300
1400
1500
1600
BROADBAND ELECTRIC
FIELD STRENGTH
E (Vm⁻¹)
10⁻²
10⁻³
10⁻⁴
10⁻⁵
APPROXIMATE WHISTLER
PEAK INTENSITIES

Figure 11

Figure 12. Upper panel: Individual whistler frequency ranges versus UT for whistlers occurring between 09:30 UT and 10:30 UT. Lower panel: Individual whistler dispersions versus UT for the time period between 09:30 UT and 10:30 UT.

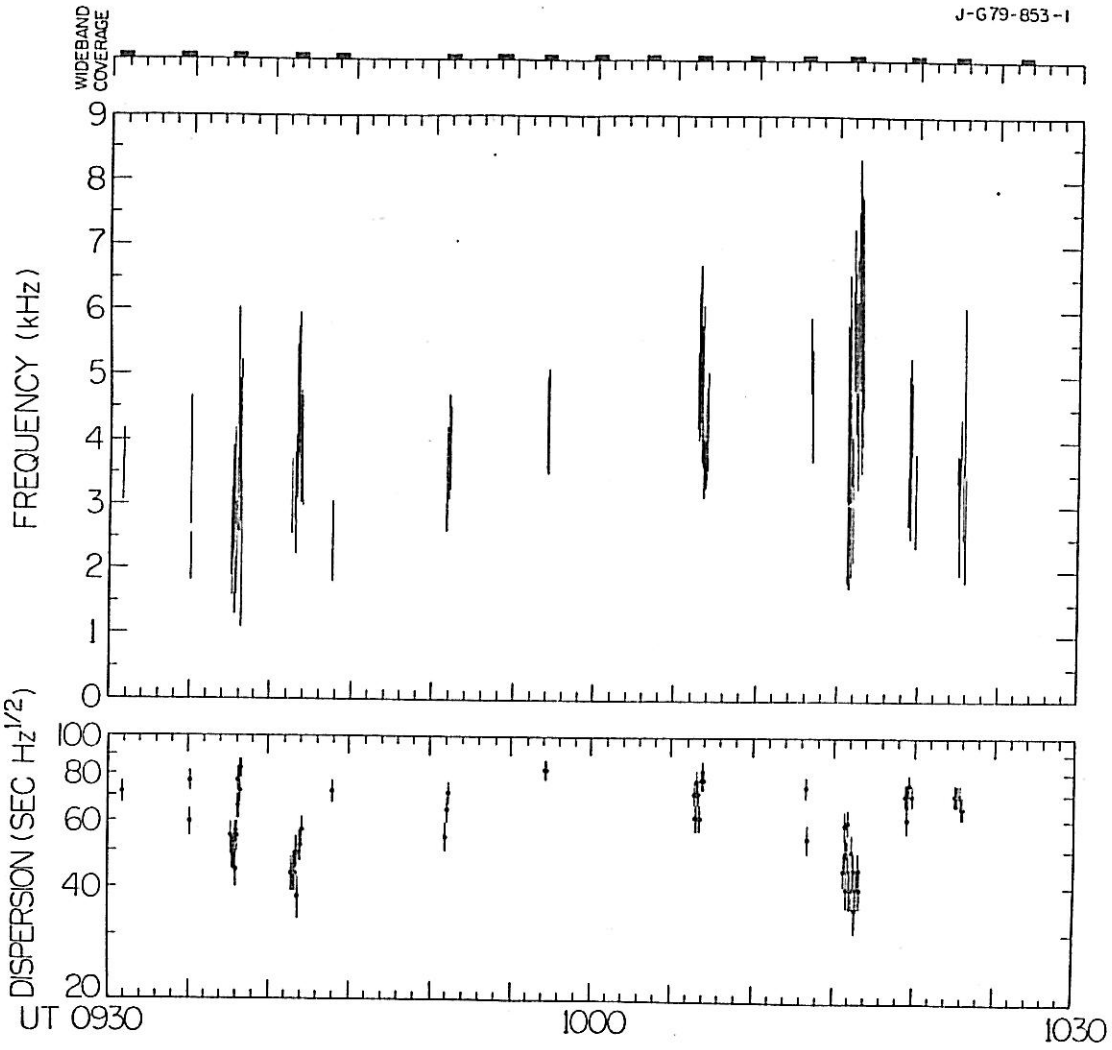
J-G79-853-1
WIDEBAND COVERAGE
FREQUENCY (kHz)
0
1
2
3
4
5
6
7
8
9
DISPERSION (SEC Hz$^{1/2}$)
20
40
60
80
100
UT 0930
1000
1030

Figure 12

REFERENCES

Acuña, M. H., and N. F. Ness, Results from the GSFC fluxgate magnetometer on Pioneer 11, in Jupiter, edited by T. Gehrels, The University of Arizona Press, Tucson, 1976, p. 836.

Bagenal, F., and J. D. Sullivan, Spatial distribution of plasma in the Io torus, Geophys. Res. Lett., 7, 41, 1980.

Broadfoot, A. L., M. J. S. Belton, B. R. Sandel, D. E. Shemansky, P. Z. Takacs, J. B. Holberg, S. K. Atrega, T. M. Donahue, H. W. Moos, J. L. Bertaux, J. E. Blamont, D. F. Strobel, J. C. McConnell, A. Dalgarno, R. Goody, and M. B. McElroy, EUV observations from Voyager 1 encounter with Jupiter, Science, 204, 979, 1979.

Cook, A. F., T. C. Duxbury, and G. E. Hunt, First results on Jovian lightning, Nature, 280, 794, 1979.

Eckersley, T. L., Musical atmospherics, Nature, 135, 104, 1935.

Gurnett, D. A., R. R. Shaw, R. R. Anderson, W. S. Kurth, and F. L. Scarf, Whistlers observed by Voyager 1: Detection of lightning on Jupiter, Geophys. Res. Lett., 6, 511, 1979.

Helliwell, R. A., Whistlers and Related Ionospheric Phenomena, Stanford University Press, Stanford, 1965, p. 35.

Kennel, C., Low frequency whistler mode, Phys. Fluids, 9, 2190, 1966.

Menietti, J. D., and D. A. Gurnett, Whistler propagation in the Jovian magnetosphere, Geophys. Res. Lett., 7, 49, 1980.

Scarf, F. L., and D. A. Gurnett, A plasma wave investigation for the Voyager mission, Space Sci. Rev., 21, 289, 1977.

Smith, B. A., L. A. Soderblom, T. V. Johnson, A. P. Ingersoll, S. A. Collins, E. M. Shoemaker, G. E. Hunt, H. Masursky, M. H. Carr, M. E. Davies, A. F. Cook II, T. Boyce, G. E. Danielson, T. Owen, G. Sagan, R. F. Beebe, J. Veverra, R. G. Strom, J. F. McCavley, D. Morrison, G. A. Briggs, and V. E. Suomi, The Jupiter system through the eyes of Voyager 1, Science, 204, 951, 1979.

Tokar, R. L., D. A. Gurnett, and R. R. Shaw, in preparation, 1981.

Warwick, J. W., J. B. Peace, A. C. Riddle, J. K. Alexander, M. D. Desch, M. L. Kaiser, J. R. Thieman, T. D. Carr, S. Gulkis, A. Boischot, C. C. Harvey, and B. M. Pederson, Voyager 1 planetary radio astronomy observations near Jupiter, Science, 204, 995, 1979.